26.1. *Hexing qingyi,* JLUM-JZ07b1 (holotype). Skull in right lateral view. L, left; R, right.

A New Basal Ornithomimosaur (Dinosauria: Theropoda) from the Early Cretaceous Yixian Formation, Northwest China

26

Jin Liyong, Chen Jun, and Pascal Godefroit*

We describe a new basal Ornithomimosauria from a specimen (JLUM-JZ07b1) discovered in the lowest beds (Lower Valanginian–Lower Barremian, Lower Cretaceous) of the Yixian Formation in western Liaoning province, P.R. China. *Hexing qingyi* gen. et sp. nov. is characterized by a series of cranial and postcranial autapomorphies: the rostral portion of the premaxilla deflected ventrally in front of the lower jaw, so that its oral surface is level with the ventral border of the dentary, a deep antorbital fossa that invades the whole lateral surface of the maxilla, a sagittal crest on the parietal, pendant paroccipital processes that extend ventrally below the level of the foramen magnum, a dentary fenestra, a phalangeal formula for manus of 0-(1 or 2)-3-3-0, and elongated (>85% length of corresponding metacarpal) proximal phalanges of digits III and IV. A phylogenetic analysis shows that *Hexing* is a basal ornithomimosaur more derived than *Pelecanimimus* but basal to *Harpymimus, Beishanglong,* and the edentulous clade formed by *Garudimimus* and the Ornithomimidae. Incomplete overlap between preserved body parts across specimens prevents full resolution of the relationships between *Hexing, Shenzhousaurus* (also from the Yixian Formation of western Liaoning province), and more advanced ornithomimosaurs. Ornithomimosauria had an extensive evolutionary history in eastern Asia from the Valanginian–Barremian, until the early Maastrichtian, and a single dispersal across the Bering Strait is required to account for the distribution of advanced Ornithomimidae in Asia and North America.

Introduction

Ornithomimosauria (ostrich-mimic dinosaurs) is a group of lightly built and cursorial theropods that are mainly known from Cretaceous localities of Asia and North America (Makovicky et al., 2004). Although phylogenetically nested among carnivorous theropods, advanced Ornithomimidae lack teeth but had beaks and gastoliths (Kobayashi et al., 1999), suggesting that their diet was completely different from that of typical theropods. Ornithomimosauria have been viewed as carnivores of small prey, insectivores, and even herbivores (Nicholls and Russell, 1981; Kobayashi et al., 1999; Makovicky et al., 2004; Barrett, 2005). They may have exhibited gregarious habits (Kobayashi and Lü, 2003; Varricchio et al., 2008).

Thousands of exceptionally preserved dinosaurs, birds, early mammals, amphibians, aquatic reptiles, pterosaurs, flowering plants, and insects have been unearthed during the last 15 years in western Liaoning province and constitute the famous Early Cretaceous Jehol Biota. Among dinosaurs,

feathered theropods from the Jehol Biota have received particular attention, allowing for the reconstruction of the early evolution of feathers and flight as well as reconstruction of the phylogenetic relationships between coelurosaurian dinosaurs and birds.

Ji et al. (2003) described *Shenzhousaurus orientalis*, the oldest known Ornithomimosauria, from the lowest more fluvial, volcanoclastic beds of Yixian Formation (Lower Valanginian–Lower Barremian; Swisher et al., 2002). Here, we describe a second ornithomimosaur from the same beds. As it is usually the case for fossils discovered in the Yixian Formation, this specimen was discovered by a local farmer, who began its preparation. The fossil was subsequently carefully prepared in the laboratory of the Geological Museum of Jilin University. All the dubious parts of the skeleton, which may have been affected by the preparation of the local farmer, have been removed and are not included in the following description.

Institutional abbreviations. CMN, Canadian Museum of Nature, Ottawa, Canada; JLUM, Geological Museum of the Jilin University, Changchun, P.R. China.

Systematic Paleontology

Dinosauria Owen, 1842
Theropoda Marsh, 1881
Tetanurae Gauthier, 1986
Coelurosauria von Huene, 1914
Ornithomimosauria Barsbold, 1976

Hexing qingyi gen. et sp. nov.
(Figs. 26.1–26.7)

Etymology. From Mandarin, *Hexing,* "like a crane," and *quingyi,* "with thin wings."

Holotype. JLUM-JZ07b1, housed in the Geological Museum of the Jilin University, Changchun (Jilin province, P.R. China).

Locality and horizon. Xiaobeigou locality, Lujiatun, Shangyuan, Beipiao City, western Liaoning province, P.R. China; lowest more fluvial, volcanoclastic beds of Yixian Formation, older than 128 million years and younger than 139 million years (Lower Valanginian–Lower Barremian; Swisher et al., 2002).

Diagnosis. Ornithomimosauria with the following autapomorphies: rostral portion of premaxilla deflected ventrally in front of lower jaw, so that its oral surface is level with the ventral border of dentary; deep antorbital fossa invades the whole lateral surface of maxilla; sagittal crest on parietal; pendant paroccipital processes that extend ventrally below the level of the foramen magnum; dentary fenestra; phalangeal formula for manus: 0-(1 or 2)-3-3-0; proximal phalanges of manus digits III and IV elongated (> 75% length of corresponding metacarpal); high (137%) hind limb ratio for tibiotarsus/femur.

Description

JLUM-JZ07b1 is incompletely preserved, including the skull, a portion of the cervical series, and most of the appendicular skeleton. All the measurements taken on JLUM-JZ07b1 are compiled in Appendix 26.1. The small size of JLUM-JZ07b1 roughly corresponds to that of juvenile *Sinornithomimus dongi* specimens, from the Upper Cretaceous of Inner Mongolia (Kobayashi and Lü, 2003). The dimensions of JLUM-JZ07b1 are also smaller than those of the holotype of the basal ornithomimid *Shenzhousaurus orientalis*, also from the Yixian formation of western Liaoning (Ji et al., 2003). However, JLUM-JZ07b1 is not a juvenile: most cranial sutures are completely fused; and complete fusion of the scapula and coracoid is present, as is fusion of the astragalus and calcaneum.

Skull. The right side of the skull is well preserved (Fig. 26.1). However,, the left side was crushed during fossilization. Palatal elements and the lateral wall of the braincase are poorly exposed. The muzzle is long and triangular, gradually tapering rostrally, and particularly slender. The skull is proportionally large when compared with other Ornithomimosauria (Table 26.1). The skull is about as long as the femur, as in *Shenzousaurus orientalis*, also from the Yixian Formation of western Liaoning province (Ji et al., 2003), although it is much shorter in other ornithomimids. However, the larger proportion of the skull in both basal ornithomimosaurs from the Yixian Formation probably mainly reflects the small size of these specimens. With a femur length of 135 mm (*Hexing*) and 181 mm (*Shenzhousaurus*), they are less than half the size of the other ornithomimosaurs taken into consideration. Further allometric studies of the ornithomimosaur skeleton should clarify this problem.

Skull openings. The whole skull is highly pneumatized (Fig. 26.1). The orbit is distinctly higher than long. The antorbital fossa is extremely developed, invading the whole lateral surface of the maxilla. The antorbital fenestra forms more than half the length of the antorbital fossa. The external narial opening is particularly small. As is usual in Ornithomimosauria (Makovicky et al., 2004), it is separated from the maxilla by the premaxillary–nasal contact. An internarial septum, as in *Harpymimus* (Kobayashi and Barsbold, 2005a), cannot be observed. The dimensions of both the supratemporal and infratemporal fenestrae cannot be measured because of lateral crushing against the lateral wall of the braincase of the postorbital and squamosal and because of the absence of the quadratojugal.

Premaxilla. The edentulous premaxilla is formed by thin nasal and maxillary processes that form the dorsal, rostral, and ventral margins of the small external opening (Fig. 26.1). The maxillary process terminates rostral to the rostral end of the antorbital fossa, as in *Shenzousaurus* (Ji et al., 2003) and *Harpymimus* (Kobayashi and Barsbold, 2005a). In more advanced Ornithomimosauria, the maxillary process extends further caudally (Kobayashi and Lü, 2003). The dorsal border of the maxillary process contacts the nasal, excluding the maxilla from the external narial opening. The rostral portion of the premaxilla, which forms the tip of the snout, is deflected ventrally in front of the rostral end of the lower jaw, so that its oral surface is level with the ventral margin of the dentary. The external surface of the premaxilla does not appear pitted by neurovascular exits that supplied

the horny beak, as it is usually observed in advanced ornithomimosaurs (Norell et al., 2001; Makovicky et al., 2004).

Maxilla. The edentulous maxilla is elongate (Fig. 26.1). Its dorsal process contact the rostral process of the lacrimal at the midpoint of the antorbital fenestra, whereas its longer ventral process contacts the jugal at the level of the caudal border of the antorbital fenestra. The exact limits between the maxilla and the nasal cannot be discerned because these bones are intimately fused together. A stout pila interfenestralis, perpendicular to the ventral process of the maxilla, forms the vertical rostral margin of the antorbital fenestra. In front of pila interfenestralis, the whole lateral surface of the maxilla is deeply excavated by the antorbital fossa. The medial wall of the anterior part of the maxillary fossa is destroyed, and it is therefore not possible to observe the presence of the maxillary and promaxillary fenestrae. The oral margin of the maxilla is sinuous. Its rostral portion is distinctly convex, corresponding to a concavity on the dorsal margin of the dentary. However, the ventral expansion of oral margin of the maxilla is not as prominent as in *Sinornithomimus, Garudimimus,* and *Gallimimus* (Kobayashi and Lü, 2003), and the oral margins of the maxilla and dentary do not form a cutting edge as this level.

Jugal. The jugal is a straplike bone that forms the ventral margin of the orbit (Fig. 26.1). Its rostral end covers the caudal end of the maxilla at the level of the antorbital bar. It resembles the condition observed in *Sinornithomimus,* but it contrasts with the bifurcated rostral end for contacts with both the maxilla and lacrimal observed in *Struthiomimus* and *Ornithomimus* (Kobayashi and Lü, 2003). Under the orbit, it becomes slightly deeper. Caudally, it bifurcates to form a caudodorsally projecting process that contacts the caudal border of the ventral process of the postorbital, as well as a short process that contacts the distal head of the quadrate. The postorbital process participates in the rostroventral border of the infratemporal fenestra and terminates below the midheight of the orbit, as usually observed in Onithomimosauria (Makovicky et al., 2004).

Nasal. The nasal is transversely narrow but rostrocaudally long: it extends from the caudal margin of the external narial opening up to the level of the midpoint of the orbit (Fig. 26.1). The nasal is slightly transversely vaulted. As is usual in ornithomimosaurs (Makovicky et al., 2004), the nasal is excluded from the dorsal margin of the antorbital fenestra by the maxilla and the lacrimal. Its caudolateral border contacts the prefrontal, and its caudal end, the frontal. Foramina on the dorsal surface of the nasal are not observed in JLUM-JZ07b1.

Lacrimal. The lacrimal is roughly T shaped (Fig. 26.1). Its long ventral process, which forms the caudal margin of the antorbital fenestra, is broken off ventrally. The caudal border of the preserved portion of the ventral process is bounded by the prefrontal along its whole height. The rostral process of the lacrimal extends forward to contact the dorsal process of the maxilla above the midpoint of the antorbital fenestra. A shorter caudal process inserts between the nasal and the prefrontal on the dorsal aspect of the skull. Close to the junction with the prefrontal, the lateral side of the lacrimal is pierced by a round foramen, also observed in *Garudimimus* and *Gallimimus* (Kobayashi and Barsbold, 2005b), and which corresponds to a caudal opening for the nasolacrimal canal.

Table 26.1. Skeletal Proportions in Selected Ornithomimosauria Genera

Taxon	Femur (mm)	Sk/F (% femur length)	H/F (% femur length)	M/F (% femur length)	T/F (% femur length)	MTIII/F (% femur length)	P/F (% femur length)
Hexing qingyi	135	101	67	76	>137	62	49
Shenzousaurus orientalis[a]	191	97	—	—	—	—	—
Sinornithomimus dongi[b]	323	57	66	—	102	66	—
Garudimimus brevipes[c]	371	68	—	—	105	62	—
Struthiomimus altus[d]	480–513	50	65–72	70–77	109–111	75–79	46–50
Ornithomimus sp.[d]	435–500	54	64	64	108–109	71–76	49
Dromiceiomimus sp.[d]	378–468	51	75	—	119–124	78–86	50–56
Gallimimus bullatus[d]	192–665	51–62	80	47	108–113	78–81	38–47

Sk/F, ratio skull length/femur length; H/F, ratio humerus length/femur length; M/F, ratio manus length (including metacarpals)/femur length; T/F, ratio tibiotarsus length/femur length; MTIII/F, ratio metatarsal III length/femur length; P/F, ratio pes length (excluding metatarsals)/femur length.
[a] Ji et al. (2003).
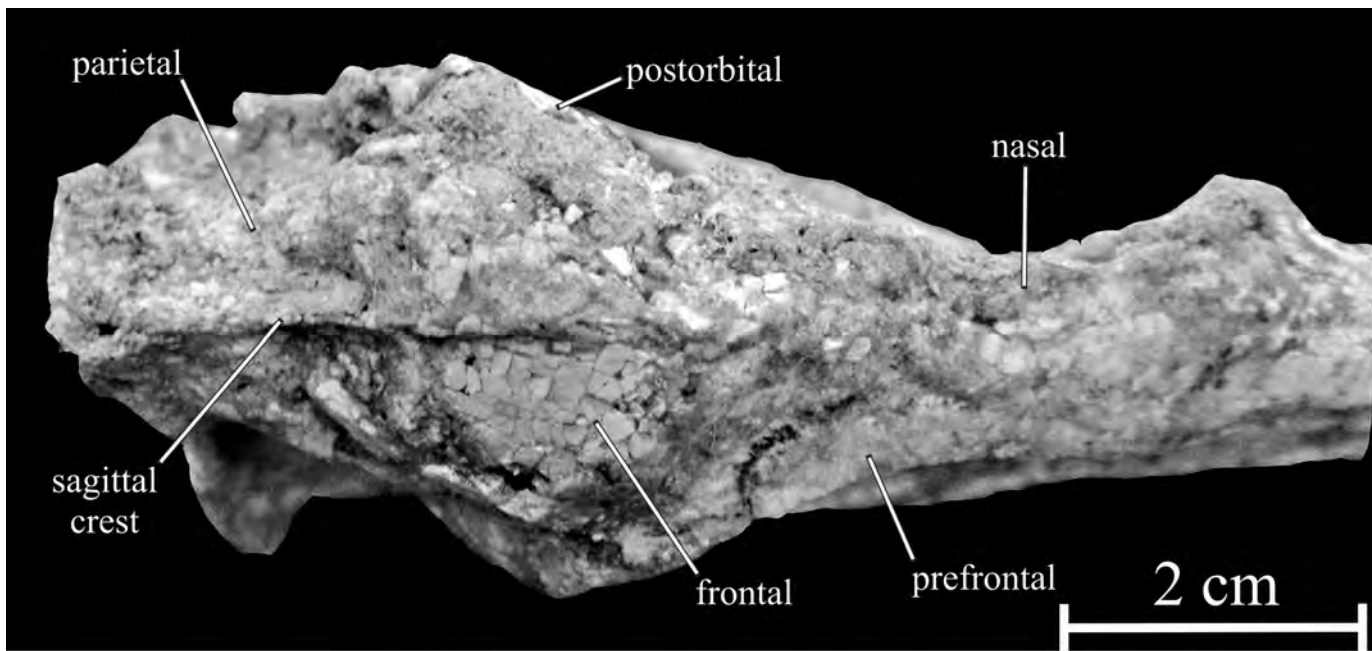[b] Kobayashi and Lü (2003).
[c] Kobayashi and Barsbold (2005b).
[d] Nicholls and Russell (1981).

Prefrontal. The prefrontal is a narrow but long curved bone that forms the rostrodorsal margin of the orbit. It starts ventrally below the midpoint of the rostral orbital margin and extends dorsally behind the midpoint of the dorsal orbital margin, well beyond the nasal (Fig. 26.1). The long ventral process of the prefrontal closely adheres to the ventral process of the lacrimal on the antorbital bar. The caudal process of the prefrontal excludes the caudal part of the nasal and he rostral part of the frontal from the orbital margin. In dorsal view, the prefrontal appears slightly larger than the lacrimal.

Frontal. The frontal of *Hexing* is relatively short, less than half the length of the nasal (Fig. 26.2). It contrasts with the situation observed in *Sinornithomimus* (Kobayashi and Lü, 2003, fig. 5), in which the frontal is only slightly shorter than the nasal. Of course, this character is likely correlated with the relative development of the snout in the different taxa. Because of the lateral crushing of the postorbital and squamosal against the lateral wall of the braincase, the lateral side of the frontal is partly obscured. However, the frontal apparently formed only a short portion of the orbital rim because of the caudal extension of the prefrontal. The planar rostral part of the frontals is sloped rostrally and meets the nasal at the midpoint of the dorsal orbital margin. As is usual in Ornithomimosauria, the frontals are domed near the caudal part of the orbit, forming a flexure between the flat rostral parts of the frontals and parietals. The paired frontals form a single dome, as in *Garudimimus* (Kobayashi and Barsbold, 2005b), but unlike *Gallimimus* (Osmólska et al., 1972) and *Sinornithomimus* (Kobayashi and Lü, 2003), which have a dome on each frontal separated by a midline depression. The caudal border of the frontal that contacts the parietal is concave. In *Shenzhousaurus* (Ji et al., 2003) and *Galliminus* (Osmólska et al., 1972), the frontoparietal suture is sinuous in dorsal view.

Parietal. As is usual in Ornithomimosauria, the parietal of *Hexing* is much shorter than the frontal (Fig. 26.2). Its rostral portion forms a wide tonguelike process that inserts between the caudal parts of the paired frontals. Contrary to other Ornithomimosauria (Ji et al., 2003; Makovicky et al., 2004), the dorsal surface of the parietal forms a well-developed sagittal crest. The parietal forms a pair of thin caudal processes that extend ventrally against the paroccipital processes. In *Garudimimus* (Kobayashi and
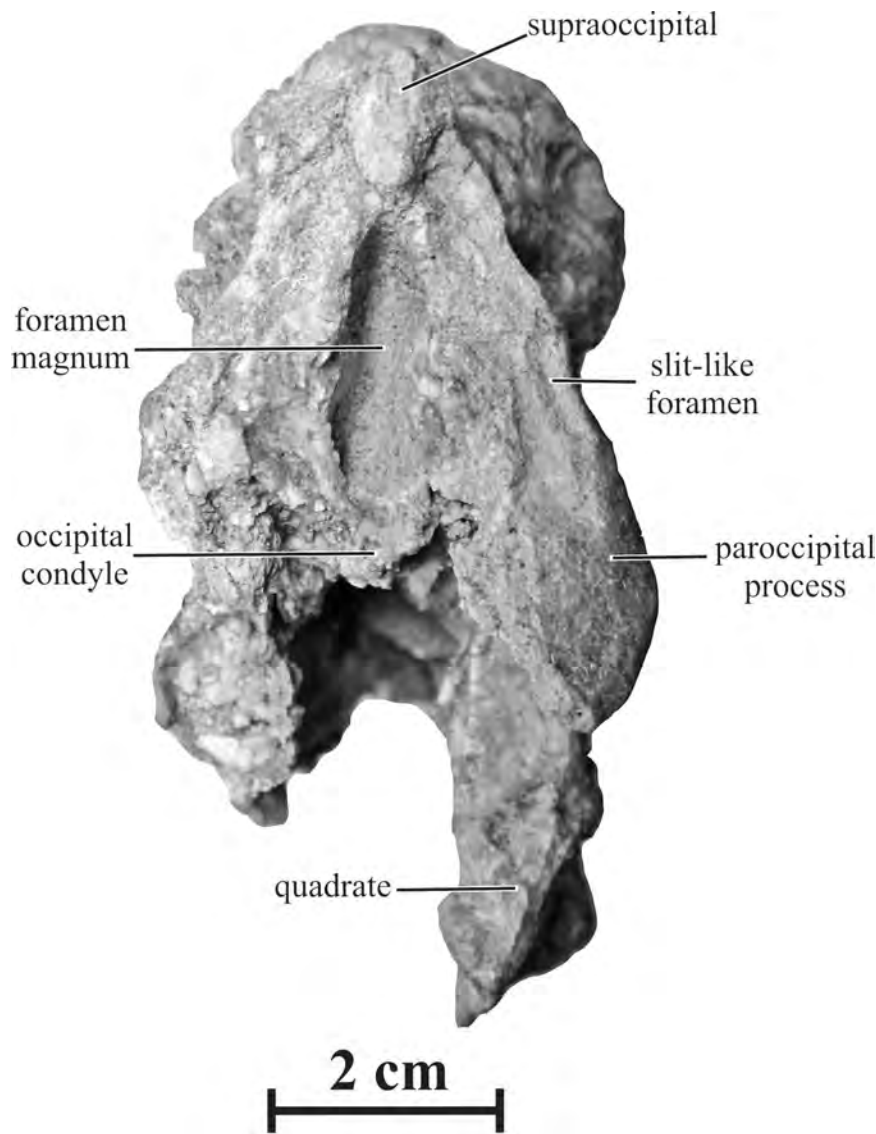
26.2. *Hexing qingyi,* JLUM-JZ07b1 (holotype). Skull roof in dorsal view.

Barsbold, 2005b) and *Sinornithomimus* (Kobayashi and Lü, 2003), these processes are straight and extend caudolaterally beyond the caudal end of the skull table.

Postorbital. The postorbital of JLUM-JZ07b1 is poorly preserved on both sides of the skull (Fig. 26.1). The rostral process is relatively short and the postorbital–frontal suture originates at the caudodorsal part of the orbit. The postorbital forms a long hooklike caudal process that participates in the intertemporal bar. The jugal process of the postorbital is long, narrow, and regularly curved, nearly forming the whole caudal margin of the orbit.

Squamosal. The complex structure of the squamosal cannot be adequately described in JLUM-JZ07b1 because this bone is completely crushed.

Caudal aspect of the skull (Fig. 26.3). The supraoccipital, exoccipitals, and opisthotics are completely fused together, and their limits cannot be discerned. The foramen magnum appears much taller than wide, but this could be due to lateral crushing of the dorsal part of the skull. Above the foramen magnum, the supraoccipital forms a prominent, dorsoventrally elongated knob. On either side of this knob, depressed areas border the dorsolateral margins of the foramen magnum. The fused exoccipitals and opisthotics form the large, pendant paroccipital processes, which extend ventrally well below the foramen magnum. They appear much more expanded ventrally than in *Gallimimus* (Osmólska et al., 1972), *Sinornithomimus* (Kobayashi an Lü, 2003, fig. 7), and *Garudimimus* (Kobayashi and Barsbold, 2005b). In any case, this unusual orientation of the processes cannot be explained by the eventual mediolateral postmortem crushing of the skull. Medially the exoccipitals border the foramen magnum. A large slitlike foramen perforates the caudal surface of the paroccipital process at midheight, close to its lateral margin. A caudal foramen on the paroccipital process can also be observed in juvenile specimens of *Gallimimus* (Makovicky et al., 2004), in *Sinornithomimus* (Kobayashi and Lü, 2003), and in *Garudimimus* (Kobayashi and Barsbold, 2005b). The medioventral portion of the caudal aspect of the paroccipital process is depressed. The

26.3. *Hexing qingyi,* JLUM-JZ07b1 (holotype). Skull in caudal view.

medioventral corner of the paroccipital process participates in the dorsal part of the occipital condyle

Quadrate. The lateral (Fig. 26.1) and caudal (Fig. 26.3) sides of the right quadrate can be observed. This bone is rather high, narrow in lateral view, and slightly curved caudally. The proximal articular head is quite simple and rounded, articulating with the squamosal. The distal head of the quadrate forms a small triangular rostrolateral process that articulates with the dorsolateral flange of the surangular just rostral to the mandibular glenoid and contacts the caudal end of the jugal. In caudal view, the fossa that encloses the quadratic foramen forms a slitlike aperture, at about midheight of the main quadrate body, close to its medial margin.

Palatine. A large, hooklike, and rostrally inclined plate inside the antorbital fenestra is interpreted as the dorsal process of the right palatine (Fig. 26.1). It appears much better developed than in other Ornithomimosauria described so far. Its lateral side bears a well-developed ridge, surrounded by triangular depressed areas.

Basioccipital. The basioccipital forms the major part of the occipital condyle. Although it is much deformed, the latter appears particularly

small, as is common in ornithomimosaurs (Kobayashi and Barsbold, 2005a). The occipital condyle has a long and slightly constricted neck, like in *Struthiomimus* (Kobayashi and Barsbold, 2005a) and the Ukhaa Tolgod ornithomimid described by Makovicky and Norell (1998). The ventral side of the basioccipital bears a strong median carina along its whole length. Between the basal tubera, the median crest forms a small tubercle, also known in the Ukhaa Tolgod ornithomimid (Makovicky and Norell, 1998). The basal tubera are moderately developed. The basisphenoid is too poorly preserved to be adequately described.
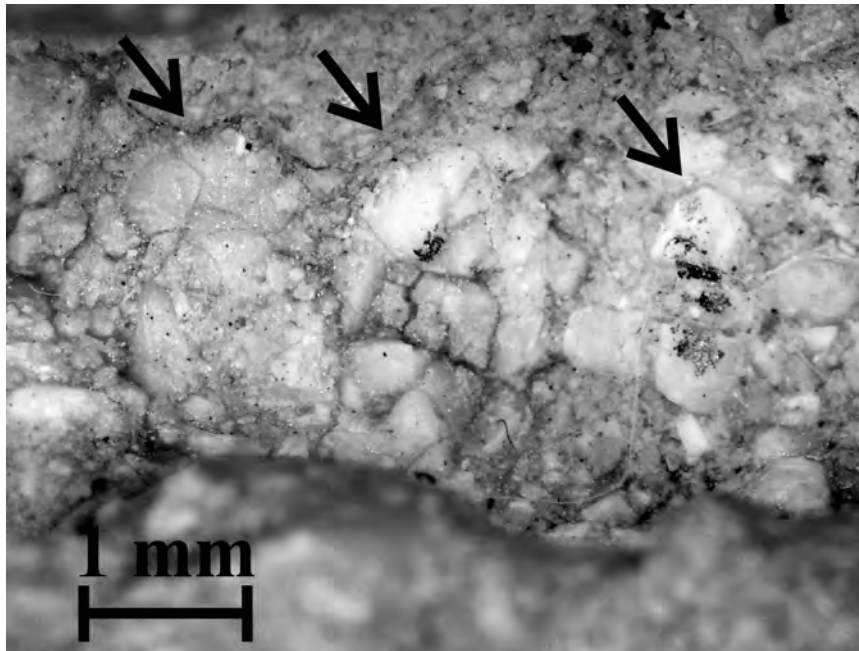
Mandible. The mandible of *Hexing* is lightly built and distinctly shorter than the skull. Its tip terminates caudal to the ventrally deflected oral surface of the premaxilla (Fig. 26.1). The large opening at the back of the mandible of JLUM-JZ07b1 is not natural but was accidentally made during the early stage of the preparation of the specimen. Indeed, the whole lateral surface of the angular and surangular is deeply excavated by a long caudal mandibular fossa and the lateral surface of both bones is therefore extremely thin and easily breakable. The "true" external mandibular fenestra begins in front of this mandibular fossa. As is usual in ornithomimosaurs, it is relatively small, extending from the level of the midheight of the orbit until the caudal third of the antorbital fenestra.

Articular. Only the lateral side of the right articular can be observed. It is trapezoidal in outline and exposed between the caudoventral border of the surangular and the caudodorsal border of the angular. It does not form a short retroarticular process that curves dorsocaudally, as observed in *Garudimimus* and Ornithomimidae (Makovicky et al., 2004).

Surangular. The lateral surface of the surangular is deeply excavated by the wide caudal mandibular fossa. Its caudodorsal border forms a small flange that extends rostrolaterally from the glenoid and articulates with the rostrolateral process on the distal head of the quadrate. This surangular flange is regarded as a synapomorphy for Ornithomimosauria (e.g., Makovicky et al., 2004). The thin rostral process of the surangular forms the dorsal margin of the external mandibular fenestra. It is overlapped by the caudodorsal process of the dentary along a short distance. Because an important part of the lateral surface of the surangular was destroyed during the early phase of the preparation of JLUM-JZ07b1, it is not possible to know whether a minute caudal foramen is present, as in *Gallimimus* and *Struthiomimus* (Makovicky et al., 2004).

Angular. The angular is slightly shorter than the surangular. If its dorsal is particularly thin because of the important development of the caudal mandibular fossa, its ventral part, which forms the caudal third of the ventral margin of the mandible, is robust. The angular and the surangular form a straight suture. They are separated caudally by the articular. Rostrally, the angular forms the caudal corner and the ventral margin of the external mandibular fenestra. The rostral process of the angular overlaps the caudoventral process of the dentary along a short distance.
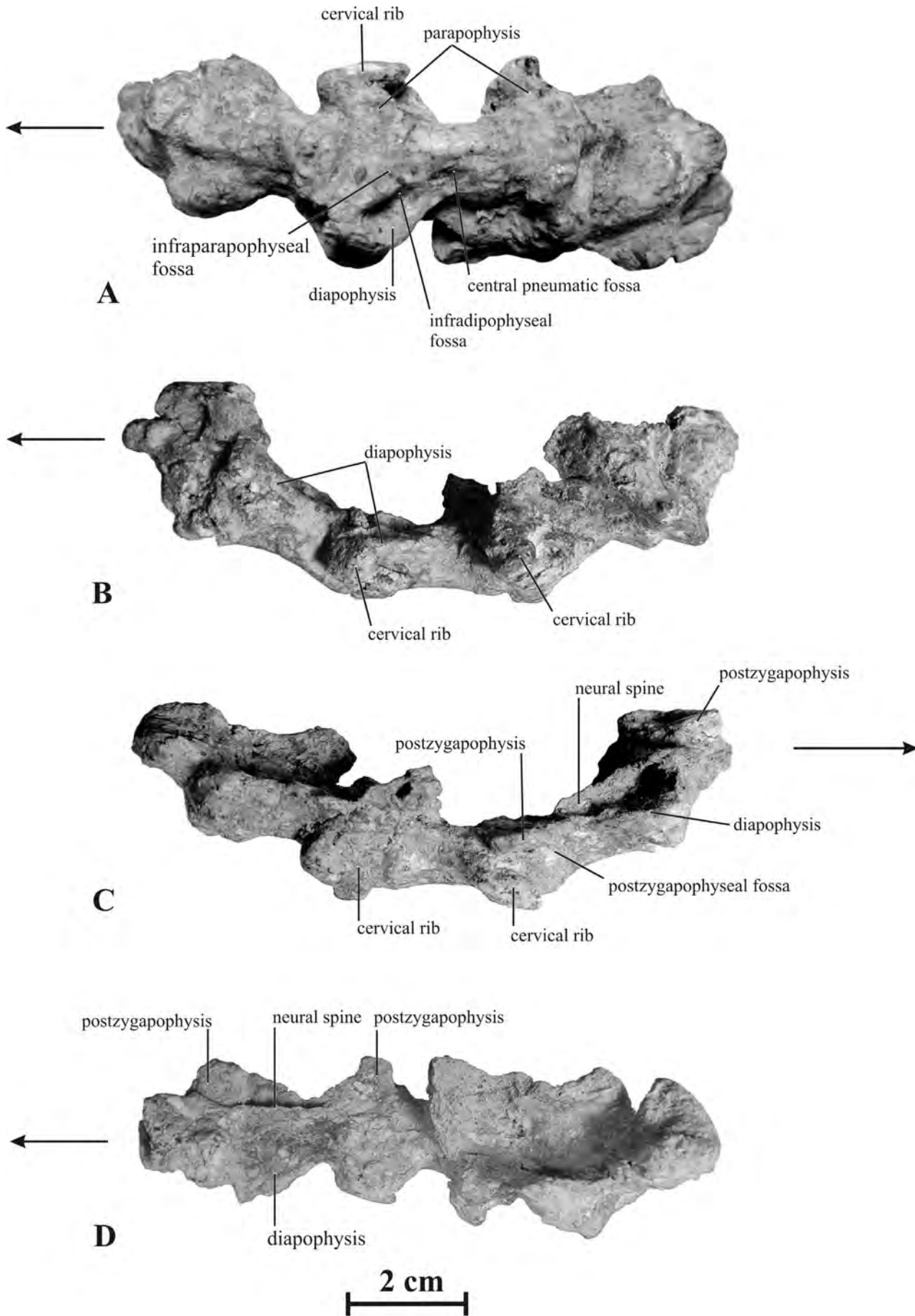
Dentary. The dentary is elongated, forming the rostral two-thirds of the lateral side of the lower jaw, and triangular in lateral view (Fig. 26.1). Its bifid caudal end forms the rostral margin of the external mandibular fenestra and contacts the surangular dorsally and the angular ventrally. The ventral edge of the dentary is perfectly straight, like in *Pelecanimimus* (Pérez-Moreno et

26.4. *Hexing qingyi,* JLUM-JZ07b1 (holotype). Detail of left dentary teeth in lingual view.

al., 1994) and *Shenzhousaurus* (Ji et al., 2003). In *Harpymimus*, the ventral edge of the dentary is gently concave (Kobayashi and Barsbold, 2005a). In other Ornithomimosauria, the ventral edge of the dentary is deflected ventrally at the level of the symphysis. Rostrally, the dorsal edge of the dentary is deflected ventrally, as in other ornithomimosaurs except *Pelecanimimus* (Ji et al., 2003). This deflection corresponds to the convex margin of the rostral part of the maxilla. However, the rostrodorsal border of the dentary does not form a cutting edge. A rostroventrally sloping elliptical fenestra pierces the lateral surface of the dentary at midlength. Because the edges of this fenestra are regular, with a finished aspect, and slightly thickened, it is unlikely that this is an artifact of preservation or a pathology. Above this fenestra, the dorsal edge of the dentary is thicker. Such aperture has not been observed in other ornithomimosaurs so far. Teeth are not preserved on the right dentary. However, three or four small conical teeth can be observed in lingual view on the rostral end of the left dentary (Fig. 26.4). They are unfortunately too poorly preserved to be adequately described.

Cervical vertebrae. Five cervical vertebrae are poorly preserved in JLUM-JZ07b1 (Fig. 26.5). The centrum is cylindrical, elongated, and dorsoventrally compressed. The diapophyses form large triangular winglike processes, attached on the lateral side of the cranial half of the centrum (Fig. 26.5D). The infradiapophyseal fossae are particularly wide below the diapophyses. Caudal to the infradiapophyseal fossa, the lateral side of the centrum has a smaller elliptical central pneumatic fossa (Fig. 26.5A). On the lateroventral sides of the centrum, the parapophyses are less expanded both craniocaudally and laterally. Cervical ribs are fused on the distal articular surfaces of the diapophyses and parapophyses (Fig. 26.5B,C). Small infraparapophyseal fossae are developed under the proximal part of the parapophyses (Fig. 26.5A). The postzygapophyses form particularly well-developed triangular winglike process, nearly symmetrical to the diapophyses on the distal half of the cervical vertebra (Fig. 26.5D). They widely cover the prezygapophyses, which consequently cannot be described. The

A — cervical rib, parapophysis, infraparapophyseal fossa, diapophysis, infradipophyseal fossa, central pneumatic fossa

B — diapophysis, cervical rib, cervical rib

C — neural spine, postzygapophysis, postzygapophysis, diapophysis, postzygapophyseal fossa, cervical rib, cervical rib

D — postzygapophysis, neural spine, postzygapophysis, diapophysis

2 cm

infrapostzygapophyseal fossa is wide and deep (Fig. 26.5A). As is usual in ornithomimosaurs, the neural spine is low (Fig. 26.5C). However, contrary to the situation in ornithomimids except *Archaeornithomimus* (Kobayashi and Lü, 2003), it remains relatively elongated and occupies more than the cranial half of the neural arch.
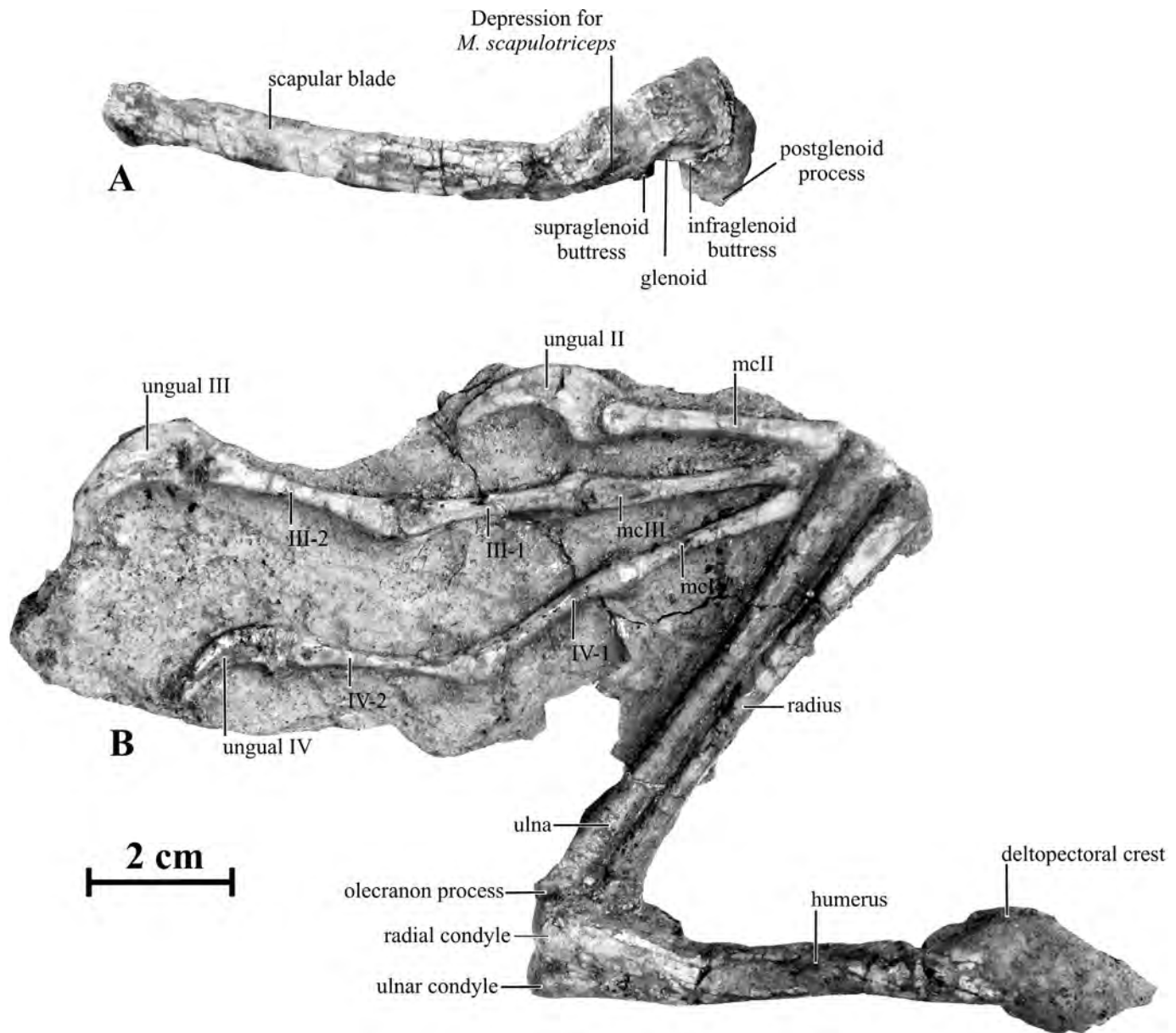
Scapula. The right scapula and coracoid are better preserved than their left counterparts. The scapula and coracoid appear fused together, and their respective limits are not easily discernable (Fig. 26.6A). This suggests that jlum-jz07b1, despite of its small size, was an adult individual. The scapula is particularly elongated and thin. It is slightly longer than the humerus, like in *Harpymimus* (Kobayashi and Barsbold, 2005a), and its blade does not expand distally. The scapular blade is gently curved cranially. The acromion process is weakly developed and truncated. The supraglenoid buttress is particularly strongly developed, and the flange of the buttress extends on the cranial surface of the scapula. Dorsal to the buttress, the depression for attachment of *M. scapulotriceps* is weakly developed. As in *Harpymimus* (Kobayashi and Barsbold, 2005a), there is a low ridge dorsal to the depression along the caudal edge of the blade. The glenoid faces posterolaterally.

Coracoid. Both coracoids are poorly preserved, and only few details can be distinguished. The postglenoid process ("posterior process" of Pérez-Moreno et al., 1994; Kobayashi and Lü, 2003) is less elongated than in *Beishanlong* (Makovicky et al., 2010), and contrary to *Harpymimus* (Kobayashi and Barsbold, 2005a), the infraglenoid buttress is much less developed than the supraglenoid buttress on the scapula (Fig. 26.6A). The infraglenoid buttress is aligned with the postglenoid process and is not offset laterally, as in some ornithomimids (Kobayashi and Lü, 2003). Although the lateral surface of the coracoid is eroded, a subglenoid shelf along the dorsal aspect of the postglenoid process, as observed in *Beishanlong* and *Archaeornithomimus* (Makovicky et al., 2010), is apparently absent.

Humerus. The humerus is slightly shorter than the scapula and slender, especially when compared with *Harpymimus* (Kobayashi and Barsbold, 2005a, fig. 6.6). Its proximal portion is partly destroyed (Fig. 26.6B). The deltopectoral crest is particularly short and weakly developed, extending distally up to one-quarter of the total length. The humeral shaft is subcircular and straight. As described in *Harpymimus,* the proximal and distal ends of the humerus are roughly aligned in the same plane, and the twist between the ends known in Late Cretaceous taxa is absent (Kobayashi and Barsbold, 2005a). Both distal condyles are about the same size. The entepicondyle (contra *Anserimus* and *Gallimimus*; Kobayashi and Lü, 2003) and ectepicondyle (contra *Beishanlong*; Makovicky et al., 2010) are not developed at all.

Ulna and radius. The forearm bones are tightly appressed along their whole length (Fig. 26.6B), indicating a limited range of pronation and supination, as is usual in Ornithomimosauria (Nicholls and Russell, 1985; Makovicky et al., 2004). The ulna and radius are only slightly shorter than the humerus. Both are particularly gracile and perfectly straight. The radius is only slightly narrower than the ulna. The olecranon appears less prominent than in other ornithomimosaurs, but it might be an artefact of preservation. The distal end of the ulna is subquadrangular in cross section,

26.5. *Hexing qingyi,* JLUM-JZ07b1 (holotype). Cervical vertebrae in ventral (A), left lateral (B), right lateral (C), and dorsal (D) views. The arrows indicate the cranial direction.

New Basal Ornithomimosaur from the Early Cretaceous Yixian Formation   477

26.6. *Hexing qingyi,* JLUM-JZ07b1 (holotype). A, Right scapulocoracoid in lateral view. B, Left humerus (caudal view), forearm (lateral view), and hand (lateral view); mc, metacarpal.

whereas the distal end of the radius is craniocaudally flattened. The distal end of the ulna extends slightly more distally than that of the radius.

Manus. We follow the nomenclature of Xu et al. (2009) for manual digits (digits II, III, and IV are preserved in Tetanurae). The manus of *Hexing* appears highly modified when compared with that in other Ornithomimosauria. Our careful preparation reveals that the left hand has not been restored at all by the local farmer who discovered the fossil and is thus trustable for description. The hand of *Hexing* is much elongated, being distinctly longer than the humerus (Fig. 26.6B), like in *Struthiomimus* (Makovicky et al., 2004). Metacarpals III and IV are similar in size and morphology: they are elongated, perfectly straight, and particularly slender. Nothing indicates that they were tightly appressed in life, contrasting with the condition observed in other ornithomimosaurs. The proximal end of metacarpals III and IV is hidden under the ulna. The distal end of the metacarpals forms a ginglymoidal surface, and there is a collateral ligament

478   *Jin et al.*

fossa on the medial side. The proximal element of digit II is elongated and slender, closely resembling metacarpals III and IV. Moreover, its distal end is slightly rotated laterally, as is usually observed on metacarpal II of ornithomimosaurs except *Harpymimus* (Kobayashi and Lü, 2003; Kobayashi and Barsbold, 2005a). For these reasons, this bone is tentatively identified as metacarpal II. However, it must be noted that in basal ornithomimosaurs, metacarpal II is a small element, approximately half or less than metacarpal III (Kobayashi and Lü, 2003; Makovicky et al., 2004); on the contrary, the first phalanx of digit II is usually the longest in the ornithomimosaur manus (Makovicky et al., 2004). Therefore, it cannot be excluded that the first element of digit II in JLUM-JZ07b1 is the first phalanx and that metacarpal II is lost.

The phalangeal formula depends on the identification of this proximal element in digit II: it is therefore 0-(1 or 2)-3-3-0. In any case, it is unique is unique among Ornithomimosauria and other basal Tetanurae (basal phalangeal formula: 0-2-3-4-0; Xu et al., 2009). It implies the disappearance probably of phalanx II-1 and of one of the phalanges in digit IV. The proximal and intermediate phalanges of digits III and IV closely resemble each other in size and morphology and are also similar with the metacarpals. All are particularly elongated and slender (length of proximal phalanx in digit III and IV >75% length of corresponding metacarpal), although the proximal phalanges of digits III and IV are usually short and robust in other ornithomimosaurs. Their distal ends have well-developed ginglymoid articulations that fit into the concave proximal surface of the adjacent phalanx. The collateral ligament fossa is also well developed on the lateral side of the distal end and faces quite laterally. The ungual phalanges are well curved in lateral view. As is usual in ornithomimosaurs (e.g., Makovicky et al., 2004), the plantar surface of the unguals is not trenchant but flattened, and it bears a small flexor tubercle distal to the proximal articulation. The groove for the claw sheath extends parallel to the plantar side of the unguals.
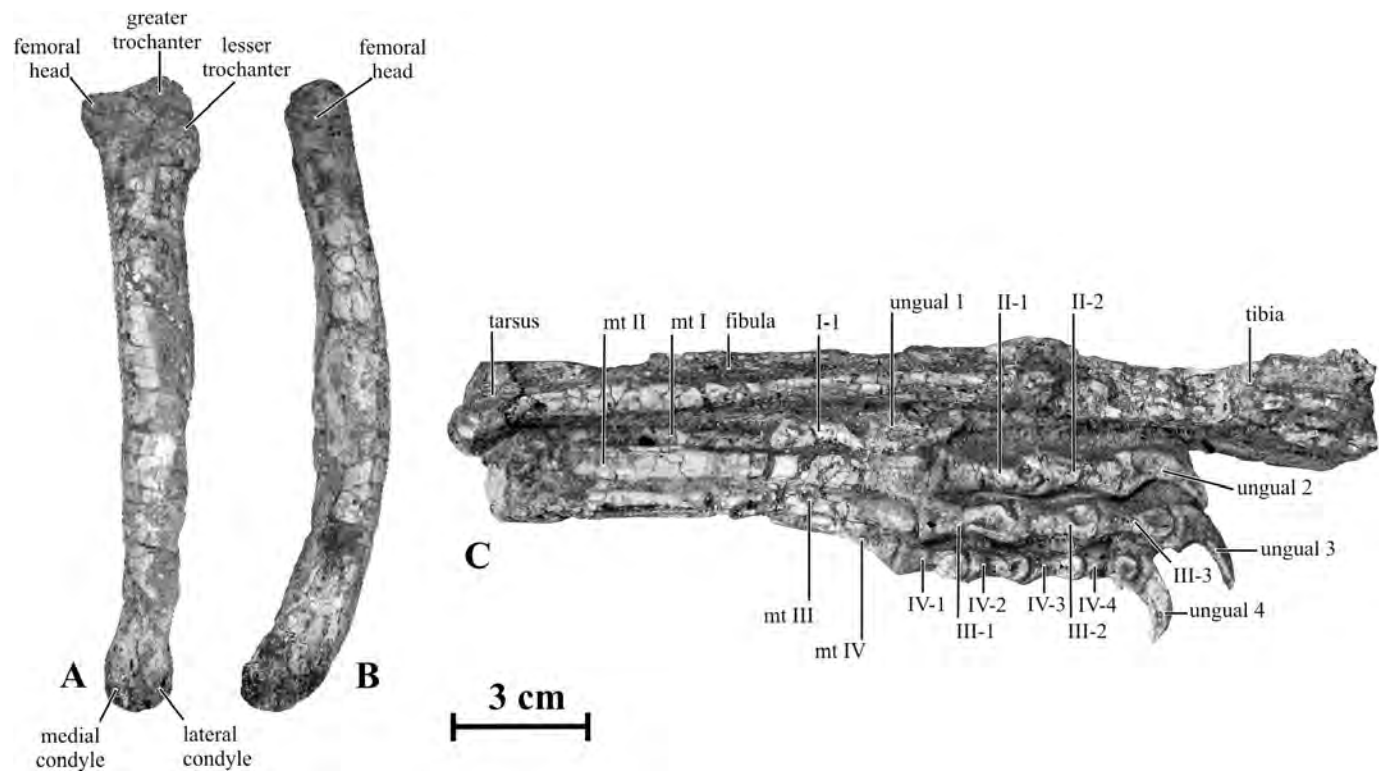
Femur. The left femur is poorly preserved in JLUM-JZ07b1, its medial side being heavily damaged (Fig. 26.7A,B). The right one was apparently restored and is therefore not described here. The femur is much shorter than the tibia. In medial view, it appears more distinctly bowed than in other Ornithomimosauria (Fig. 26.7B). The partially preserved lesser trochanter is alariform and robust; it is placed more laterally than the greater trochanter (Fig. 26.7A). A rounded ridge divides the lesser trochanter into cranially and caudally oriented surfaces. The apex of the greater trochanter is rounded. It lateral side is extensively depressed, delimited cranially by the lesser trochanter, and caudally by a low poorly preserved proximodistally extending ridge. The distal end of the femur is slightly enlarged mediolaterally and the medial condyle appears better developed than the lateral condyle (Fig. 26.7A).

Tibiotarsus and fibula. The right tibia and fibula are also poorly preserved and cannot be adequately described. The tibia, fibula, and astragalus are completely fused together (Fig. 26.7C), suggesting that this specimen was an adult individual. The tibia and fibula appear elongated and slender. The hind limb ratio for tibiotarsus/femur is more than 137%—much higher than in other Ornithomimosauria (Table 26.1). However, it cannot be excluded that this character is size related among ornithomimosaurs. Indeed,

Currie (1998) shows that juvenile tyrannosaurids have proportionally longer tibiae than older individuals: bivariate comparisons of tibial versus femoral lengths indicate an important negative allometry of the tibia length during growth. Although Nicholls and Russell (1981, table 2) indicate that the hind limb ratio for tibiotarsus/femur varies between 108–109 in larger *Ornithomimus* specimens (femur lengths 435–500 mm), this ratio is much higher (147) in a smaller *Ornithomimus* individual (CMN 8636, femur length 310 mm; Currie, 1998, table 2). It is therefore possible that smaller ornithomimosaurs taxa have proportionally longer tibiae than larger individuals and that the elongated tibia in the small JLUM-JZ07b1 mainly reflects this negative allometry. Of course, this statement uses intraspecific scaling relations to extrapolate interspecific scaling, which is a weak justification; further allometric investigations in ornithomimosaurs would help in clarifying this situation. The distal end of the fibula articulates with the lateral side of the tibia, whereas it is placed on the cranial side of the tibia in some advanced ornithomimids. The astragalus is firmly attached to the distal part of the tibia, and the calcaneum is imperceptibly fused with the astragalus.

Metatarsals. Both metatarsal I and digit I are preserved in JLUM-JZ07b1, like in *Garudimimus* (Kobayashi and Barsbold, 2005b). There is no trace of a metatarsal V, as it is also preserved in the latter taxon, but it might be an artifact of preservation. The reduction of metatarsal I is not as drastic as in *Garudimimus,* in which it only one fifth of the length of metatarsal III (Kobayashi and Barsbold, 2005b). Although it is incompletely preserved in JLUM-JZ07b1, it is a bit more than half of the length of metatarsal III (Fig. 26.7C). Metatarsals II and III have nearly the same size, while metatarsal IV is a bit shorter. In contrast to the tibia, the metatarsals appear relatively short when compared with the femur. According to Kobayashi and Barsbold (2005b), a relatively low (<0.7) hind limb ratio for metatarsal III/femur can be observed in other Asian ornithomimids, including *Sinornithomimus, Anserimimus, Garudimius,* and also some *Gallimimus* specimens (although this ratio seems highly variable in the latter) and appears to be the retention of ancestral nonornithomimosaur theropod metatarsal proportions for taxa of that body size (Holtz, 1994). Kobayashi and Barsbold (2005b) also observed that metatarsal proportions are apparently not size related among ornithomimosaurs. The proximal end of metatarsal III is well exposed in cranial view, as in basal ornithomimosaurs. It is slightly mediolaterally compressed when compared with the proximal end of metatarsal II. Although it is incompletely preserved, the lateral side of metatarsal IV looks shallowly concave. A deep collateral ligament fossa is developed on the medial side of metatarsal I. The distal surfaces of the metatarsals look only slightly convex.

Pedal phalanges. The pes phalangeal formula is 2-3-4-5-0 (Fig. 26.7C). The proportions of the foot are similar to those in other ornithomimosaur in which they can be measured (Table 26.1). Digit III is the longest, while the second and the fourth toes are subequal in length. All proximal and intermediate phalanges closely resemble each other. Their size decreases distally and the phalanges from the fourth toe are smaller than those from digits I to III (Appendix 26.1). Like in *Harpymimus,* the intermediate phalanges remain relatively long in comparison with the proximal ones, whereas they are proportionally much shorter in *Garudimimus* and ornithomimids.

26.7. *Hexing qingyi,* JLUM-JZ07b1 (holotype). Left femur in cranial (A) and medial (B) views. C, Left tibiotarsus, fibula and pes (elements exposed in various views); mt, metatarsal.

For example, phalanx II-2 is 81% of the length of II-1, which is much longer than phalanx II-2 in ornithomimids (<60%; Kobayashi and Lü, 2003). The distal surfaces of the phalanges (except the unguals) apparently form ginglymoidal articulations. The collateral ligament fossa is deep on the lateral side of the distal articular surface. The ungual of digit II is the longest, but it appears slightly less recurved than on the third toe. As in other ornithomimosaurs, the plantar surface of the unguals is flat. Like in *Harpymimus* (Kobayashi and Barsbold, 2005a), the flexor tubercle is well developed on the caudal part of the ventral surface of the pedal unguals.

Phylogenetic Analysis

We undertook a numerical cladistic analysis of Ornithomimosauria in order to resolve the phylogenetic position of *Hexing*. This phylogenetic analysis is based on the matrix of Kobayashi and Lü (2003). However, a few characters were slightly modified, and nine supplementary characters, culled from Nicholls and Russell (1981), Ji et al. (2003), Makovicky et al. (2004, 2010), and Kobayashi and Barsbold (2005a) have been added to the original matrix (see Appendix 26.2). The data matrix (Appendix 26.3) was analyzed using PAUP*4.0b10 (Swofford, 2000), with Branch and Bound search, and both with accelerated (ACCTRAN) and delayed (DELTRAN) transformations. The analysis produced nine most parsimonious trees of 71 steps, with CI = 0.69, RI = 0.82, and RC = 0.57. The strict consensus tree is presented in Fig. 26.8, and the tree description appears in Appendix 26.4. It must be noted that character 28 (length of metacarpal II: approximately half of less than metacarpal III [0], slightly shorter [1] or longer [2]; Kobayashi and Lü, 2003) was coded as 1 for *Hexing,* assuming that the proximal element in digit II is metacarpal II. However, the general topology of the consensus tree does not change when character 28 is coded as 0 in *Hexing.*
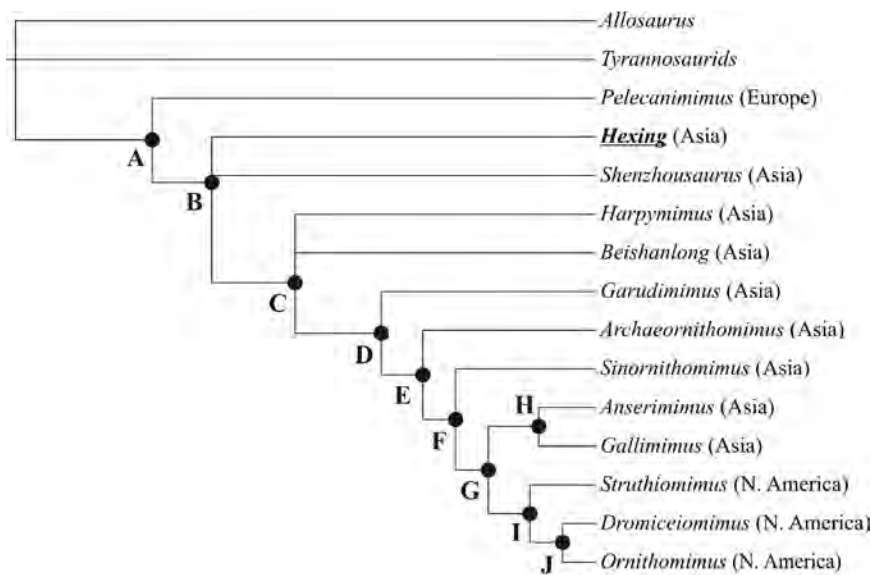
This cladogram of course closely resembles that obtained by Kobayashi and Lü (2003), but it is also perfectly compatible with those recovered by Ji et al. (2003) and Makovicky et al. (2010), and there is thus a general consensus concerning the phylogeny of Ornithomimosauria. *Pelecanimimus*, from the late Barremian of Calizas de la Huergina Formation (Cuenca, Spain: Pérez-Moreno et al., 1994; see Chapter 22 in this book), retains plesiomorphic states such as an upper dentition (characters 1 and 3), a prominence on the lateral surface of the lacrimal (character 6), and a straight dorsal edge of the dentary (character 39). This analysis also posits *Hexing* as a basal ornithomimosaur more derived than *Pelecanimimus* but basal to *Harpymimus*, from the Shinekhudag Svita (Late Albian) of Mongolia (Kobayashi and Barsbold, 2005a), *Beishanlong*, from the Xinminpu Group (Aptian–Albian) of Gansu province in China (Makovicky et al., 2010), and the edentulous clade formed by *Garudimimus* and Ornithomimidae. Incomplete overlap between preserved body parts across specimens prevents full resolution of relationships between *Hexing*, *Shenzhousaurus*, also from the Yixian Formation of western Liaoning province, and more derived ornithomimosaurs. *Hexing* and *Shenzhousaurus* are particularly small ornithomimosaurs. As in *Hexing* and *Harpymimus*, the manus digit II of *Shenzhousaurus* is apparently much smaller than digits III and IV. However, because only the ungual phalanx is preserved in digit II, it cannot be decided whether this shortening results from shortening of metacarpal II, like in *Harpymimus*, or loss of the proximal phalanx, as in *Hexing*.

Harpymimus, *Beishanlong*, and the edentulous clade share the following unambiguous (that diagnose a node under both ACCTRAN and DELTRAN optimization) synapomorphies: rostral portion of the ventral edge of the dentary deflected ventrally (character 9), presence of two antorbital fenestrae (character 16), sigmoid ischial shaft (character 44), proximal end of metatarsal III partly or completely covered by metatarsals II and IV (character 37), and truncated postacetabular process of ilium (character 45). *Garudimimus*, from the Bayanshiree Svita (Cenomanian–Campanian: Makovicky et al., 2004), and Ornithomimidae are characterized, for example, by the complete loss of their dentition (character 10). The phylogeny of Ornithomimosauridae has already been discussed in detail by Kobayashi and Lü (2003); North American Ornithomimidae (*Strutiomimus*, *Dromiceiomimus*, and *Ornithomimus*) are apparently monophyletic and are best characterized by the strongly convex ventral border of their pubic boot, with ventral expansion (character 35).

Paleogeographic Implications

With a presumed Early Valanginian to Early Barremian age, *Hexing* and *Shenzhousaurus*, from the lower beds of the Yixian Formation of western Liaoning province, are the oldest known ornithomimosaurs. *Pelecamimimus*, from the Calizas de la Huergina Formation of Cuenca (Spain), is the most primitive ornithomimosaur known so far but is Late Barremian in age (Pérez-Moreno et al., 1994; see Chapter 22 in this book). This temporal paradox indicates that the place for origin of Ornithomimosauria (Europe or Asia?) remains conjectural. Whatever it may be, the presence of basal ornithomimosaurs in western Europe and eastern Asia during the

26.8. Cladogram of Ornithomimosauria, showing the phylogenetic relationships of *Hexing qingyi*. Letters correspond to nodes defined in Appendix 26.4.

Barremian indicates that connections between Europe and Asia through the Turgai Straight were already established, well before the Aptian (contra Doré, 1991; Russell, 1993; Smith et al., 1994).

Examining distributions within the context of the phylogeny (Fig. 26.8) reveals that ornithomimids have an extensive evolutionary history, from the Valanginian–Barremian until the Early Maastrichtian, in eastern Asia, as also described for Iguanodontoidea (see also Chapters 19 and 20 in this book). With the exception of *Pelecanimimus* and of the doubtful *Timimus* from the Eumeralla Formation (Early Albian) of Dinosaur Cove (Victoria, Australia: Rich and Vickers-Rich, 1994), recently reidentified as a Dromaeosauridae? indet. cf. Unenlaiinae (Agnolin et al., 2010), all Early Cretaceous ornithomimosaurs have been discovered in Eastern Asia. The oldest ornithomimid is *Sinornithomimus*, from the Ulansuhai Formation (early Late Cretaceous according to Kobayashi and Lü, 2003, but Aptian–?Albian according to Makovicky et al., 2004) of Inner Mongolia (China) and the most primitive representative of this clade, is *Archaeonithomimus*, from the Iren Dabasu Formation (Turonian–Coniacian according to Averianov, 2002, but Early Maastrichtian according to Van Itterbeeck et al., 2005) of Inner Mongolia. The three North American ornithomimosaurid genera are Late Campanian and Maastrichtian in age. Because they are regarded as monophyletic, a single dispersal across the Bering Strait is required to account for their distribution. Because ornithomimids have not been reported yet from older Late Cretaceous strata in North America, Makovicky et al. (2004) hypothesized that ornithomimids may have dispersed less readily across the Bering Strait than did clades such as hadrosaurids and pachycephalosaurs.

Ornithomimosaurs have recently been reported in Europe on the basis of a fragmentary humerus discovered in Late Maastrichtian marine deposits from Bulgaria (Mateus et al., 2010). However, this identification is uncertain, and the presence of ornithomimosaurs in Upper Cretaceous deposits from Europe, following the separation of Asia and Europe by the Turgai Strait after the Albian (Smith et al., 1994), therefore remains speculative.

Appendix 26.1. Measurements taken on JLUM-JZ07b1

L, left; R, right.

Skull: length: 136 mm
    maximum height: 53 mm
Orbit (R): length: 31.5 mm
    height: 37.8 mm
Snout: length (rostral point of
    orbit–tip of premaxilla):
    80 mm
Antorbital fossa (R): length: 55 mm
Antorbital fenestra (R): length:
    29.5 mm
    Height: 24 mm
External naris (R): length: 7 mm
Mandible (R): length: 115 mm
Scapula (R): length: ~104 mm
    height at distal end: 10 mm
    height of proximal plate:
    14 mm
Humerus (L): length: ~90 mm
    width at deltopectoral crest:
    19 mm
    width at distal end: 16 mm
Ulna (L): length: 81 mm
    width at distal end: 9 mm
    height (craniocaudal diameter)
    at distal end: 9 mm
Radius (L): length: ~76 mm
    height (craniocaudal diameter)
    at distal end: 6 mm
    width at distal end: 10 mm
Manus (L): length: ~103 mm
"Metacarpal II" (L): length: 33 mm
    proximal height: 4.5 mm
Metacarpal III (L): length: > 31
    mm
Metacarpal IV (L): length: > 30
    mm
Manual ungual II (L): length:
    22 mm
    proximal height: 8.5 mm
Manual phalanx III-1 (L): length:
    25 mm
    proximal height: 5 mm
Manual phalanx III-2 (L): length:
    26 mm
    proximal height: 5 mm

Manual ungual III (L): length:
    23 mm
    proximal height: 9 mm
Manual phalanx IV-1 (L): length:
    23 mm
    proximal height: 4.5 mm
Manual phalanx IV-2 (L): length:
    24 mm
    proximal height: 5 mm
Manual ungual IV (L): length:
    18 mm
    proximal height: 7 mm
Femur (L): length: 135 mm
Tibia (R): length: >185 mm
Metatarsal II (R): length: 86 mm
Metatarsal III (R): length: 84 mm
Metatarsal IV (R): length: ~79 mm
Pes phalanx I-1 (R): length: 23 mm
Pes ungual I (R): length: 21 mm
Pes phalanx II-1 (R): length: 22 mm
    proximal height: 9 mm
Pes phalanx II-2 (R): length: 18 mm
    proximal height: 8 mm
Pes ungual II (R): length: 20 mm
    proximal height: 9 mm
Pes phalanx III-1 (R): length:
    18 mm
    proximal height: 9 mm
Pes phalanx III-2 (R): length: 16 mm
    proximal height: 7.5 mm
Pes phalanx III-3 (R): length: 15 mm
    proximal height: 7.5 mm
Pes ungual III (R): length: 16 mm
    proximal height: 9 mm
Pes phalanx IV-1 (R): length:
    13.5 mm
    proximal height: 7 mm
Pes phalanx IV-2 (R): length: 13 mm
    proximal height: 6 mm
Pes phalanx IV-3 (R): length: 12 mm
    proximal height: 6 mm
Pes phalanx IV-4 (R): length: 12 mm
    proximal height: 6 mm
Pes ungual IV (R): length: 16 mm
    proximal height: 7.5 mm

The following list only includes characters that have been modified from Kobayashi and Lü (2003) or that are not included in Kobayashi and Lü's (2003) original matrix.

Appendix 26.2. Character List

9. Ventral edge of dentary: straight (0), or rostral portion reflected ventrally (1).
37. Proximal end of metatarsal III: completely exposed in cranial view (0), subarctometatarsal metatarsus (1), or arctometatarsal metatarsus (2). Character treated as ordered.
39. Dorsal edge of dentary: straight (0), or rostral portion concave resulting in a gap between upper and lower jaws when jaws are closed (1).
40. Retroarticular process of mandible: deflected ventrally (0), or curved caudodorsally (1) (Makovicky et al., 2004).
41. Surangular flange: absent (0) or present (1) (Makovicky et al., 2004).
42. Proximal and distal ends of humerus: in the same plane (0), or twisted (1). (Kobayashi and Barsbold, 2005a).
43. Radius and ulna: well separated distally (0), or closely appressed distally (1) (Nicholls and Russell, 1985; Makovicky et al., 2004).
44. Ischial shaft: straight (0), or sigmoid (1) (Ji et al., 2003).
45. Postacetabular process of ilium: gently curved (0), or truncated (1) (Ji et al., 2003).
46. Medial expansion of metatarsal III diaphysis: absent (0), or present (1) (Makovicky et al., 2010).
47. Pedal unguals: curved (0), or straight (1) (Makovicky et al., 2010).

Characters 1–38: see Kobayashi and Lü (2003, appendix 1), characters 9 and 37 modified—see Appendix 26.1; characters 39–47: see Appendix 26.1.

Appendix 26.3. Data Matrix

```
Allosaurus         00000 00000 00000 00000 00000 00000 00000
                   00000 00000 00
Tyrannosaurids     00010 00000 00000 00000 00000 10000 ?0000
                   02000 00000 00
Pelecanimimus      0?0?? 0?100 10??? 0?1?1 ????1 ??110 111??
                   ???00 101?? ??
Hexing             1011? 10?00 10101 ?1?01 ?1001 10110 ?01??
                   00010 101?? 00
Shenzhousaurus     10111 1??00 10??? 0???? ????? ????? ??110
                   ???10 1??00 ??
Harpymimus         10111 10?10 10101 1110? 01001 10000 0110?
                   ?1010 10111 00
Beishanlong        ????? ????? ????? ????1 01001 10??0 ??1??
                   010?? ?011? 00
Garudimimus        11111 11111 11111 11?0? ????? ????? ???00
                   01111 1???1 10
Archaeornithomimus ????? ????? ????? ???01 01001 20110 1?110
                   ?2??? ??111 11
Sinornithomimus    11111 11111 111?0 1?111 00001 20110 11100
                   12111 11111 11
Anserimimus        ????? ????? ????? ???11 10100 21211 01100
                   121?? ?1?1? 1?
Gallimimus         11111 11111 11100 00111 11101 21111 11100
                   12111 11111 11
```

```
Struthiomimus    11110  01?11  11110  11111  01001  ?0111  11101
                 12111  11111  11
Dromiceiomimus   1111?  11?11  1??10  1???1  00011  10???  ??101
                 12111  11?11  11
Ornithomimus     11110  11?11  11111  11111  00011  20211  11101
                 12111  11111  11
```

Appendix 26.4. Tree Description

The "describetrees" option of PAUP*4.0b10 was used to interpret character state transformations. All transformations are based upon the derivative strict reduced consensus tree (see Fig. 26.8). Transformation was evaluated under accelerated transformation (ACCTRAN) and delayed transformation (DELTRAN) options; unambiguous synapomorphies are those that diagnose a node under both ACCTRAN and DELTRAN optimization. Node numbers refer to Fig. 26.8. For simple 0–1 state changes, only the character number is given; for other state changes, the type of change is specified in parentheses.

Node A (Ornithomimosauria): Unambiguous: 8, 11, 18, 20, 25, 28, 29, 33, 41, 43; ACCTRAN: 5, 13, 15, 17, 22, 32.
Node B: Unambiguous: 1, 3, 6, 39; DELTRAN: 5.
Node C: Unambiguous: 9, 16, 37, 44, 45; DELTRAN: 32.
Node D: Unambiguous: 2, 7, 10, 12, 38, 40, 46; ACCTRAN: 14, 26, 42.
Node E (Ornithomimidae): Unambiguous: 37 (1 to 2), 47; ACCTRAN: 15, 36; DELTRAN: 26, 31.
Node F: Unambiguous: 19; ACCTRAN: 22 (1 to 0); DELTRAN: 15 (1 to 0), 36, 42.
Node G: Unambiguous: 30.
Node H: Unambiguous: 21, 23, 27; ACCTRAN: 14 (1 to 0), 16 (1 to 0), 17 (1 to 0).
Node I: Unambiguous: 5 (1 to 0), 35; DELTRAN: 14.
Node J: Unambiguous: 24; ACCTRAN: 28 (0 to 2); DELTAN: 22 (1 to 0).

Acknowledgments

The authors are grateful to P. J. Makovicky for reviewing an earlier version of this paper and making useful recommendations.

References

Agnolin, F. L., M. D. Ezcurrah, D. F. Pais, and S. W. Salisbury. 2010. A reappraisal of the Cretaceous non-avian dinosaur faunas from Australia and New Zealand: evidence for their Gondwanan affinities. Journal of Systematic Palaeontology 8: 257–300.

Averianov, A. O. 2002. An ankylosaurid (Ornithischia: Ankylosauria) braincase from the Upper Cretaceous Bissekty Formation of Uzbekistan. Bulletin de l'Institut royal des Sciences naturelles de Belgique, Sciences de la Terre 72: 97–110.

Barrett, P. M. 2005. The diet of ostrich dinosaurs (Theropoda: Ornithomimosauria). Palaeontology 48: 347–358.

Barsbold, R. 1976. On the evolution and systematics of the late Mesozoic dinosaurs. Paleontologi i biostratigrafi Mongolii, Sovmestna Svetsko–Mongolska Paleontologiceska Ekspedici Trudy 3: 68–75.

Currie, P. J. 1998. Possible evidence of gregarious behavior in tyrannosaurids. Gaia 15: 271–277.

Doré, A. G. 1991. The structural foundation and evolution of Mesozoic seaways between Europe and the Arctic. Palaeogeography, Palaeoclimatology, Palaeoecology 87: 441–492.

Gauthier, J. A. 1986. Saurischian monophyly and the origin of birds; pp. 1–55 in K. Padian (ed.), The origin of birds and

the evolution of flight. Memoirs of the California Academy of Sciences 8.

Holtz, T. R., Jr. 1994. The phylogenetic position of Tyrannosauridae: implication for theropod systematic. Journal of Paleontology 68: 1100–1117.

Huene, F. von. 1914. Das natürliche System der Saurischia. Zentralblatt für Mineralogie, Geologie und Paläontologie B 1914: 69–82.

Ji, Q., M. A. Norell, P. J. Makovicky, K.-Q. Gao, S. Ji, and C. X. Yuan. 2003. An early ostrich dinosaur and implications for ornithomimosaur phylogeny. American Museum Novitates 3420: 1–19.

Kobayashi, Y., and R. Barsbold. 2005a. Reexamination of a primitive ornithomimosaur, *Garudimimus brevipes* Barsbold, 1981 (Dinosauria: Theropoda), from the Late Cretaceous of Mongolia. Canadian Journal of Earth Sciences 42: 1501–1521.

———. 2005b. Anatomy of *Harpymimus okladnikovi* Barsbold and Perle 1984 (Dinosauria: Theropoda) of Mongolia; pp. 97–126 in K. Carpenter (ed.), The carnivorous dinosaurs. Indiana University Press, Bloomington.

Kobayashi, Y., and J.-C. Lü. 2003. A new ornithomimids dinosaur with gregarious habits from the Late Cretaceous of China. Acta Palaeontologica Polonica 48: 235–259.

Kobayashi, Y., J.-C. Lü, Z.-M. Dong, R. Barsbold, Y. Azuma, and Y. Tomida. 1999. Palaeobiology: herbivorous diet in an ornithomimid dinosaur. Nature 402: 480–481.

Makovicky, P. J., and M. A. Norell. 1998. A partial ornithomimids braincase from Ukhaa Tolgod (Upper Cretaceous, Mongolia). American Museum Novitates 3247: 1–16.

Makovicky, P. J., Y. Kobayashi, and P. J. Currie. 2004. Ornithomimosauria; pp. 137–150 in D. B. Weishampel, P. Dodson, and H. Osmólska (eds.), The Dinosauria. 2nd ed. University of California Press, Berkeley.

Makovicky, P. J., D. Li, K.-Q. Gao, M. Lewin, G. M. Erickson, and M. A. Norell. 2010. A giant ornithomimosaur from the Early Cretaceous of China. Proceedings of the Royal Society B 277: 191–198.

Marsh, O. C. 1881. Classification of the Dinosauria. *American Journal of Science* (ser. 3) 23: 81–86.

Mateus, O., G. J. Dyke, N. Motchurova-Dekova, J. D. Kamenov, and P. Ivanov. 2010. The first record of a dinosaur from Bulgaria. Lethaia 43: 88–94.

Nicholls, E. L., and A. P. Russell. 1981. A new specimen of *Struthiomimus altus* from Alberta with comments on the classificatory characters of Upper Cretaceous ornithomimids. Canadian Journal of Earth Sciences 18: 518–526.

Norell, M. A., P. J. Makovicky, and P. J. Currie. 2001. The beaks of ostrich dinosaurs. Nature 412: 873–874.

Osmólska, H., E. Roniewicz, and R. Barsbold. 1972. A new dinosaur, *Gallimimus bullatus* n. gen., n. sp. (Ornithomimidae), from the Upper Cretaceous of Mongolia. Palaeontologica Polonica 27: 103–143.

Owen, R. 1842. Report on British fossil reptiles. Part 2. Report of the British Association for the Advancement of Science (Plymouth) 11: 60–204.

Pérez-Moreno, B. P., J. L. Sanz, A. D. Buscalioni, J. J. Moratalla, F. Ortega, and D. Rasskin-Gutman. 1994. A unique multitoothed ornithomimosaur dinosaur from the Lower Cretaceous of Spain. Nature 370: 363–367.

Rich, T. H., and P. Vickers-Rich. 1994. Neoceratopsians and ornithomimosaurs: dinosaurs of Gondwanan origin? National Geographic Research and Exploration 10: 129–131.

Russell, D. A. 1993. The role of Central Asia in dinosaurian biogeography. Canadian Journal of Earth Sciences 30: 2002–2012.

Smith, A. G., D. G. Smith, and B. M. Funnell. 1994. Atlas of Mesozoic and Cenozoic coastlines. Cambridge University Press, Cambridge, 99 pp.

Swisher, C. C., III, X. Wang, Z. Zhou, Y. Wang, F. Jin, J. Zhang, X. Xu, F. Zhang, and Y. Wang. 2002. Further support for a Cretaceous age for the feathered-dinosaur beds of Liaoning, China: new ^{40}Ar/^{39}Ar dating of the Yixian and Tuchengzi Formations. Chinese Science Bulletin 47: 135–138.

Swofford, D. L. 2000. Phylogenetic Analysis Using Parsimony (and other methods). Version 4.0b10. Sinauer Associates, Sunderand, Mass., 40 pp.

Van Itterbeeck, J., D. J. Horne, P. Bultynck, and N. Vandenberghe. 2005. Stratigraphy and palaeoenvironment of the dinosaur-bearing Upper Cretaceous Iren Dabasu Formation, Inner Mongolia, People's Republic of China. Cretaceous Research 26: 699–725.

Varricchio, D. J., P. C. Sereno, X.-J. Zhao, L. Tan, J. A. Wilson, and G. H. Lyon. 2008. Mud-trapped herd captures evidence of distinctive dinosaur sociality. Acta Palaeontologica Polonica 53: 567–578.

Xu, X., J. M. Clark, J. Mo, J. Choiniere, C. A. Forster, G. M. Erickson, D. W. E. Hone, C. Sullivan, D. A. Eberth, S. Nesbitt, Q. Zhao, R. Hernandez, C.-K. Jia, F.-L. Han, and Y. Guo. 2009. A Jurassic ceratosaur from China helps clarify avian digital homologies. Nature 459: 940–944.